

A METHOD FOR IMPEDANCE IDENTIFICATION OF GRID

A Project Report

submitted by

RAVITEJA GAYATRI

*in partial fulfilment of the requirements
for the award of the degree of*

**BACHELOR OF TECHNOLOGY
&
MASTER OF TECHNOLOGY**



**DEPARTMENT OF ELECTRICAL ENGINEERING
INDIAN INSTITUTE OF TECHNOLOGY MADRAS.**

JUNE 2013

CERTIFICATE

This is to certify that the project report titled **A METHOD FOR IMPEDANCE IDENTIFICATION OF GRID**, submitted by **RAVITEJA GAYATRI**, to the Indian Institute of Technology, Madras, for the award of the degree of **BACHELOR OF TECHNOLOGY & MASTER OF TECHNOLOGY**, is a bonafide record of the project work done by him under our supervision. The contents of this report, in full or in parts, have not been submitted to any other Institute or University for the award of any degree or diploma.

Prof. Krishna Vasudevan
Guide
Professor
Dept. of Electrical Engineering
IIT-Madras

Place: Chennai

June 28, 2013

ACKNOWLEDGEMENTS

I am very grateful to my guide Prof. Krishna Vasudevan, for the guidance, motivation and valueble words during the project period.

I am also grateful lab-mates, wingmates and close-friends Abhishek, Ashwathy, Bharath, Deekshit, Jeshma, Kashyap, Madhuri, Mukul, Rahul, Rakesh, Ramesh, Raviteja, Rohit, Vikas and Zubair, who have been constantly supporting and giving moral boost to me at all times in the project. I would also like to thank Sugunakar, who spent his valueble time to help me in my project.

Finally, I would like to thank my parents, sister and family for bearing with my rants during the highs and lows of the project and for their constant show of support, faith and encouragement.

ABSTRACT

KEYWORDS: Weak Grid, Impedance, X/R Ratio, MATLAB

Weak Grid is a grid which has short-circuit capacity lower than the load demand. Due to increase in renewable energy generation, the number of weak grids in operation have increased. The attempt here is to identify whether a grid is weak or not. It is found that X/R ratio of a grid can determine whether the grid is weak or not. For this reason, the problem is tackled by using a method used to identify the impedance of a given grid. A method used to identify the grid is implemented in MATLAB and verified by changing the grid impedance values. For the identification of impedance, different disturbances are created and generated and are successfully used to identify impedance of a grid.

TABLE OF CONTENTS

ACKNOWLEDGEMENTS	i
ABSTRACT	ii
LIST OF TABLES	v
LIST OF FIGURES	viii
ABBREVIATIONS	ix
NOTATION	x
1 INTRODUCTION	1
1.1 Objective	1
1.2 Organization of Report	1
2 CLASSIFICATION OF GRIDS	2
2.1 Types of Grids	2
2.1.1 Strong Grid	2
2.1.2 Weak Grid	3
2.1.3 Micro Grid	3
2.2 Weak Grid and its characterization	4
2.2.1 Properties of Weak Grid	4
2.2.2 Characterization of Weak Grid	5
3 IMPEDANCE IDENTIFICATION PROCESS	7
3.1 Method used for identification	7
3.1.1 Derivation of expression	8
3.2 Signal Processing	12
4 SIMULATION FOR IMPEDANCE IDENTIFICATION OF GRID	13
4.1 Simulation Parameters	13

4.2	Simulation for a simple RL load	14
4.2.1	System results registered and Impedance Plots	14
4.2.2	Method Verification	16
4.3	Simulations for LC parallel load	19
4.3.1	System results registered and Impedance Plots	20
4.3.2	Method Verification	21
4.4	Simulations for Permanent Magnet DC Motor	22
4.4.1	System results registered and Impedance Plots	23
4.4.2	Method Verification	24
4.5	Simulation for a Three-bus System	26
4.5.1	System results observed	27
4.5.2	Method Verification	27
5	SIMULATION OF SYSTEM DISTURBANCES AND POWER QUALITY MEASUREMENT	30
5.1	Simulation of Voltage Swell	30
5.2	Simulation of Voltage Sag	31
5.3	Simulation for disturbance by adding sudden RL load to a DC motor system	33
6	CONCLUSIONS	35
6.1	Conclusion	35
6.2	Future Work	35

LIST OF TABLES

5.1	Voltages and current <i>THD</i> percentages during normal operation and during swell	31
5.2	Voltages and current <i>THD</i> percentages during normal operation and during sag	32
5.3	Voltages and current <i>THD</i> percentages during normal operation and when loaded with extra RL load	33

LIST OF FIGURES

2.1	Strong Grid: Voltage and frequency unaffected by load	3
2.2	Weak Grid: Voltage is affected by the load	3
2.3	Micro Grid: Both voltage and frequency are affected by the load . .	3
2.4	Weak Grid Droop Characteristics in comparison to Strong Grid . . .	4
3.1	Equivalent model of system and load voltage/current signals	8
3.2	Equivalent circuit used for analysis	9
3.3	Equivalent circuit with harmonic generating device	9
3.4	Effective circuit when switch S_1 is off	9
3.5	Effective circuit when switch S_1 is on	10
4.1	Circuit used for simulation	14
4.2	Voltage-time plot for RL load	15
4.3	System current-time plot for RL load	15
4.4	Frequency response of real and reactive source impedance values for RL load	15
4.5	System with capacitor installed across the PCC	16
4.6	Frequency Response of real and reactive source impedance values with Capacitive filter at the PCC	17
4.7	Thevenin equivalent impedance of system as seen by load	17
4.8	Ideal Frequency Response of real and reactive source impedance values for capacitive filter	18
4.9	System with LC filter installed across the PCC	18
4.10	Frequency Response of real and reactive source impedance values with LC filter at the PCC	18
4.11	Thevenin equivalent impedance of system as seen by load	19
4.12	Frequency Response of impedance magnitude ideal plot with LC filter at the PCC	19
4.13	System with load as parallel combination of inductor and capacitor .	20
4.14	Voltage and current differences during disturbance vs time	20

4.15	Frequency Response of real and reactive source impedance values for LC load	20
4.16	LC load with capacitor at PCC	21
4.17	Frequency response of real and reactive source impedance values for LC load with capacitor at PCC	21
4.18	LC load with capacitor at PCC	22
4.19	Frequency response of real and reactive source impedance values for LC load with LC filter at PCC	22
4.20	System loaded with a PMDC machine	23
4.21	Voltage-time plot of system loaded with PMDC motor	23
4.22	System-side current vs time plot for system loaded with PMDC motor	23
4.23	Frequency response of real and reactive source impedance values for system loaded with PMDC machine	24
4.24	DC machine loaded system with capacitor at PCC	24
4.25	Frequency response of real and reactive source impedance values for system loaded with PMDC motor	25
4.26	DC machine loaded system with LC filter at PCC	25
4.27	Frequency Response of real and reactive source impedance values for system loaded with PMDC machine and LC filter at PCC	26
4.28	Single line model of three-bus system used for simulation	26
4.29	Simulation circuit for the three-bus system	27
4.30	Frequency Response of source resistance for three-bus system	27
4.31	Frequency Response of source reactance for three-bus system	27
4.32	Simulation circuit for verification of correctness of impedance for three-bus	28
4.33	Frequency Response of real and reactive source impedance for capacitive loading at PCC	28
4.34	Ideal Frequency Response of real and reactive source impedance for capacitor loading at PCC	28
4.35	Frequency Response of real and reactive impedance for LC loading at PCC	29
4.36	Ideal Frequency Response of real and reactive source impedance for LC loading at PCC	29
5.1	Voltage swell caused by sudden decrease of load	30
5.2	Current change caused by voltage swell	30
5.3	Frequency response of impedance found by using voltage swell method	31

5.4	Voltage sag caused by sudden decrease of load	32
5.5	Current change caused by voltage sag	32
5.6	Frequency response of impedance found by using voltage sag method	32
5.7	Voltage change caused by sudden RL switching on motor load . . .	33
5.8	Current change caused by sudden RL switching on motor load . . .	33
5.9	Frequency response of impedance found by sudden RL switching on motor load	34

ABBREVIATIONS

IITM	Indian Institute of Technology, Madras
SCC	Short Circuit Capacity
SCR	Short Circuit Ratio
xrr	X/R Ratio
PCC	Point of Common Coupling
KCL	Kirchoff's Current Law
KVL	Kirchoff's Voltage Law
RHS	Right Hand Side
DFT	Discrete Fourier Transform
FFT	Fast Fourier Transform
PMDC	Permanent Magnet Direct Current
THD	Total Harmonic Distortion

NOTATION

U	Voltage, V
i	Current, A
Z	Impedance, Ω
R	Resistance, Ω
X	Reactance, Ω
L	Inductance, H
C	Capacitance, F

CHAPTER 1

INTRODUCTION

The present scenario in power systems has a dire requirement for increase in power generation from renewable sources, which are solar and wind power. The power generated by these generators is not constant and keeps varying in intensity according to the conditions present. The power grids which are connected using these kind of sources are called weak grids. In weak grids, due to high ohmic value of source impedance due to design restrictions, there is a significant drop in voltage when power is delivered to the load.

By taking advantage of the ohmic characteristics of weak grid, the aim of project is to identify the impedance of a grid, which will help in identification of a weak grid from distribution point of view. Another aspect studied in the project is change in power quality due to different disturbances which can occur in a grid.

1.1 Objective

The objective of project is to identify a method used for identification of grid impedance, and to find a method which can use grid impedance to identify whether the grid is weak.

1.2 Organization of Report

Chapter 2 gives a brief introduction to grids an insight into how grids are classified.

Chapter 3 explains the method used for identifying the impedance of a grid.

Chapter 4 shows simulations done on impedance identification of grid and tests done to verify the correctness of method used.

Chapter 5 is about how different disturbances occur in a grid and brief power quality analysis for the disturbances.

Chapter 6 gives conclusion and scope for future work

CHAPTER 2

CLASSIFICATION OF GRIDS

Grid is an interconnected network of sources, loads and transmission lines which transmits power from supplier to the consumer. It can be split into three parts

- **Generation:** Generating stations generate electrical power to be supplied to loads.
- **Transmission:** Transmission lines are high voltage lines which carry electrical power from generators to consumers.
- **Distribution:** Distribution system is referred to load centers where the electrical power is consumed.

2.1 Types of Grids

From the prospective of load, grids are classified depending on whether the load affects the grid voltage and frequency as follows :

- Strong Grid
- Weak Grid
- Micro Grid

2.1.1 Strong Grid

A grid is generally referred to as an ideal strong grid when the the grid voltage and frequency are independent of the nature of load, and the current drawn by the load. However, in reality we can define strong grid as a grid in which there is minimal affect of load and current drawn by the load on grid voltage and frequency.

Strong grid can be characterized as a grid which has short-circuit capacity much greater than the load size, i.e. current drawn by the load.

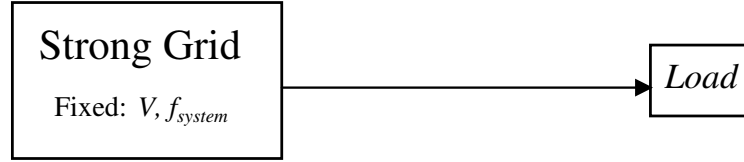


Figure 2.1: Strong Grid: Voltage and frequency unaffected by load

2.1.2 Weak Grid

A grid is referred to as weak grid when the short-circuit capacity of the system is less than the load demand. Generally, as the size of weak grid is large, frequency of grid can still be considered fixed even for small changes in local load.

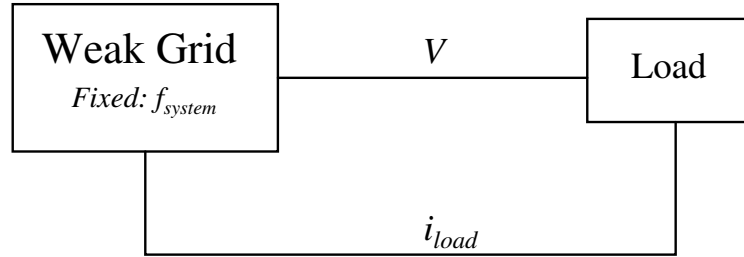


Figure 2.2: Weak Grid: Voltage is affected by the load

2.1.3 Micro Grid

Micro-grids are generally referred to loads which are kept in operation when connected from the main grid by locally generated power matching the load. In this system, the power generators have low short-circuit capacity and are used for low voltage, for example an inverter providing power to a house when there is power outage. Hence, load can affect both voltage and frequency of the system.

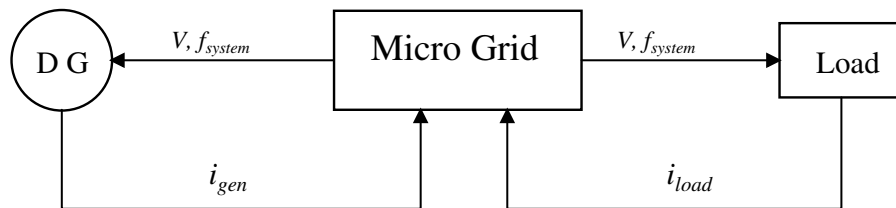


Figure 2.3: Micro Grid: Both voltage and frequency are affected by the load

2.2 Weak Grid and its characterization

2.2.1 Properties of Weak Grid

The following figure shows the voltage-current characteristics of different grids and loads.

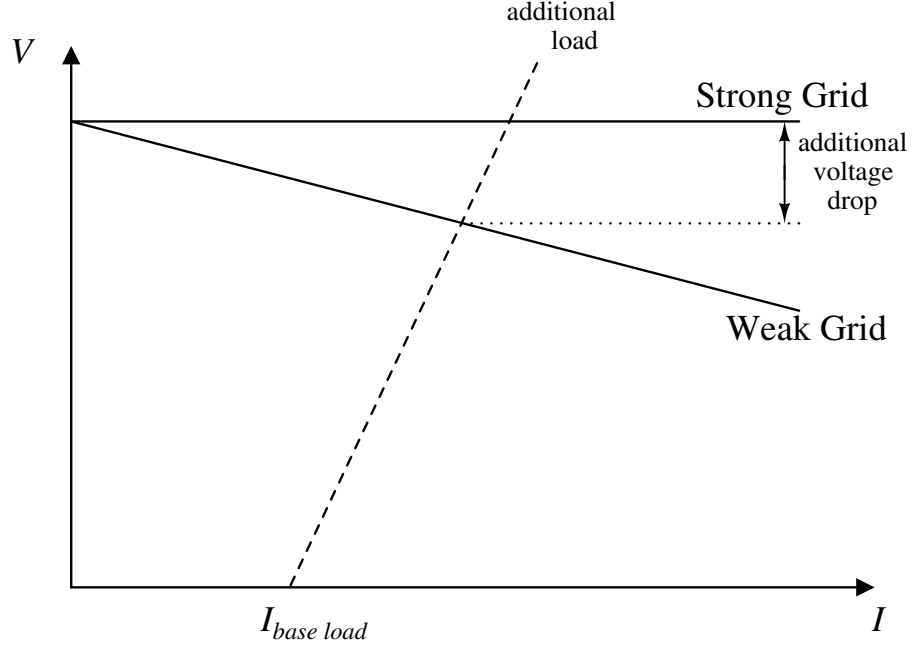


Figure 2.4: Weak Grid Droop Characteristics in comparison to Strong Grid

In figure 2.4, solid line refers to voltage-current characteristics of source and dotted line refers to voltage-current characteristics of load. The point of intersection of the two characteristics gives the operation point of the grid. As we can see from the figure, strong grid has a flat voltage-current characteristics whereas in a weak grid, current drawn from grid causes a voltage drop, which is a droop function at the point of common coupling (*PCC*), where the slope depends on the grid impedance and the power factor of load (Bollen *et al.* (2005)).

The relation between voltage drop and the load current is as shown in equation 2.1

$$\Delta U = (R_s \cos \phi + X_s \sin \phi) I \quad (2.1)$$

where

$\Delta U = \text{Voltage drop at the PCC}$

$R_s = \text{Grid Resistance as seen from PCC}$

$X_s = \text{Grid Reactance as seen from PCC}$

$\phi = \text{Power Factor of load}$

$I = \text{Current flowing through the load}$

2.2.2 Characterization of Weak Grid

A grid can be characterized by different parameters. Beneath its voltage level and its total power capability the short circuit capacity (SCC) can be defined. The SCC is the amount of power flowing at a given point in case of a short circuit. It is mainly dependent on the rated voltage, U_G and the absolute value of grid impedance Z_s , which can be measured at this point. The grid impedance is the sum of impedances of many grid components and typically differs from region to region. One part of it consists of the impedance of the transmission line itself which mainly depends on material, diameter and length of the line. Transformers are used to connect lines with different voltage levels. They are typically high inductive. To reduce the burden of the grid from reactive power flows and to stabilize it, special compensation devices are installed which are typically capacitive in nature. And different loads make a big contribution towards the grid impedance as well. They can change during the day and can have ohmic, inductive or capacitive character (Grunau *et al.* (2012)).

If an active load with rated power of S_R is connected to the grid and grid impedance is assumed to be Z_s , short circuit ratio SCR can be defined as shown in equation 2.2

$$SCR = \frac{SCC}{S_R} = \frac{U_G^2}{Z_s S_R} \quad (2.2)$$

If SCR of a grid is smaller than 10, the grid is considered as a weak grid Strachan *et al.* (2010).

Grid can also be characterized by the ratio of reactive and ohmic parts of the grid

impedance Z_s , called $\frac{X}{R}$ ratio(xrr). With the help of grid impedance and xrr , the reactive amount X_s and ohmic amount R_s can be calculated from equations 2.3 and 2.4.

$$X_s = \frac{Z_s}{\sqrt{1 + (\frac{1}{xrr})^2}} \quad (2.3)$$

$$R_s = \frac{Z_s}{\sqrt{1 + (xrr)^2}} \quad (2.4)$$

Weak grids typically have a low xrr , such as 0.5, so they have an ohmic character.

CHAPTER 3

IMPEDANCE IDENTIFICATION PROCESS

There are various methods to identify grid impedance and each method has its own advantages and disadvantages. The main aim is to achieve accurate measurement of grid impedance in frequency spectrum for atleast fifteen to twenty harmonics which will significantly help in power quality analysis of the grid as well.

The most important problem faced in impedance identification is that there is no freedom to turn-off and turn-on the grid whenever there is a requirement for measurement of impedance. So impedance identification measurements have to be done on-line.

The method presented in this chapter is aimed at identifying grid impedance for the purpose of identifying a grid as a weak grid. Hence, these methods may not work well for identifying grid impedance of all kinds of grids but will definitely work efficiently for identification of a weak grid.

3.1 Method used for identification

From the impedance identification point of view, there is no significant difference between the system and its load, except for the system ability to deliver energy at the fundamental frequency. Equivalent harmonic sources in the system and the load linear models can be situated either in the system side or the load side of the *PCC*, with different contributions to the observed voltage in the accessible cross-section (figure 3.1).

By using different current measurements $i_{sys}(t)$ and $i_{load}(t)$ as shown in figure 3.1, it is possible to identify source impedance as well as load admittance. In general, as $|Z_{load}(\omega)| \gg |Z_s(\omega)|$, the disturbed current will mainly flow through system side and hence, source impedance identification is easier (Staroszczyk (2005)).

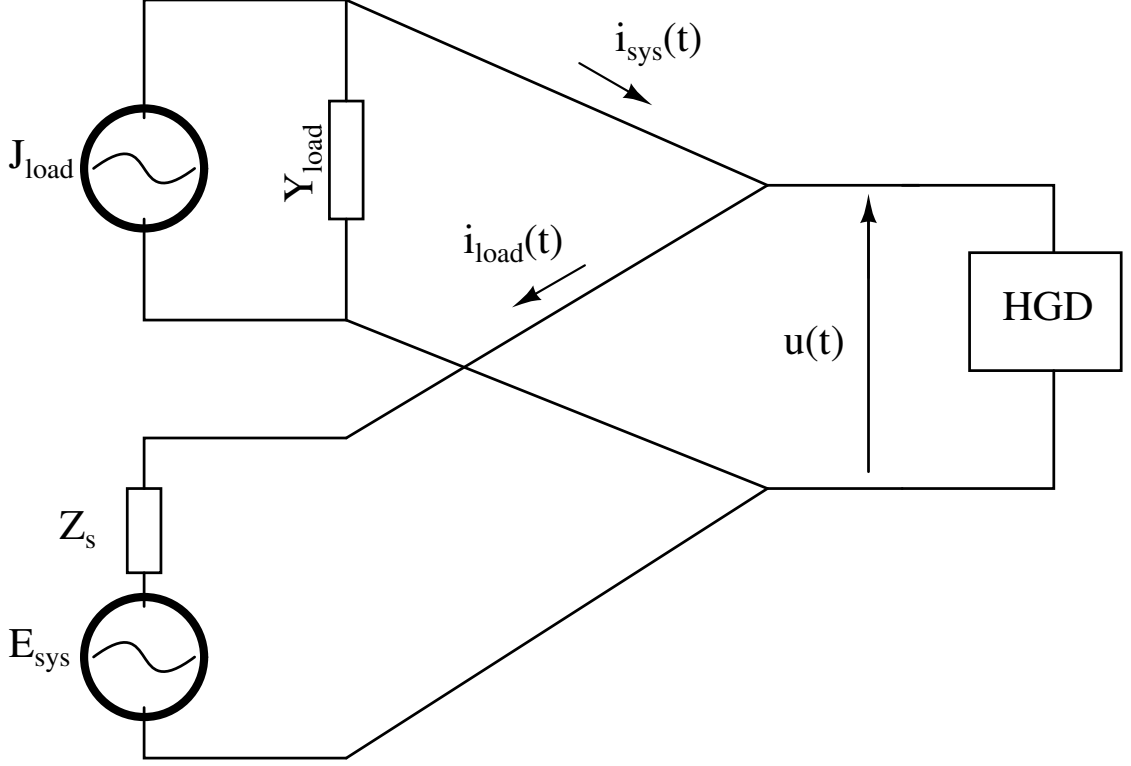


Figure 3.1: Equivalent model of system and load voltage/current signals

There is no measurement problem in direct signal ($i(t)/u(t)$) observations, so the knowledge of source impedance $Z_s(\omega)$ and load admittance $Y_{load}(\omega)$ fully describes the linear model of the system. But as the requirement is the identification of source impedance $Z_s(\omega)$, identification methods for load admittance are not discussed further.

The method for identification can be divided into two parts as follows:

- Generation of harmonics and measurement of signals
- Processing the acquired signals and identifying source impedance from the measurements.

3.1.1 Derivation of expression

To obtain the expression for source impedance, a simple circuit consisting of a voltage source with rms voltage V and source impedance $R_s + jX_s$ is considered. This source is connected to a load with load impedance Z_l as shown in figure 3.2. For finding out the effective source impedance, system is injected with harmonic currents by using simple low impedance short for a short time at the *PCC*, which in this case is the node which connects source impedance and load.

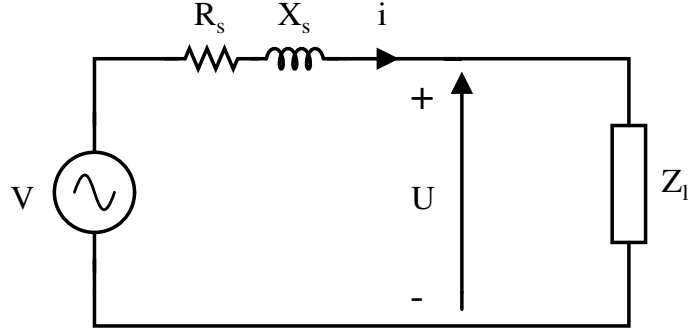


Figure 3.2: Equivalent circuit used for analysis

For the circuit shown in figure 3.2, by adding the short-circuit impedance Z_{sc} and switch S_1 at the *PCC*, the circuit will look as shown in figure 3.3.

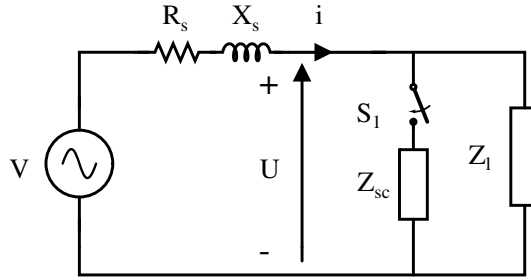


Figure 3.3: Equivalent circuit with harmonic generating device

The circuit shown above has two modes of operation:

- Switch S_1 is off
- Switch S_1 is on

The figure below shows the circuit diagram when switch S_1 is off. Voltage at the *PCC* and system current when switch S_1 is off are assigned U_1 and i_1 .

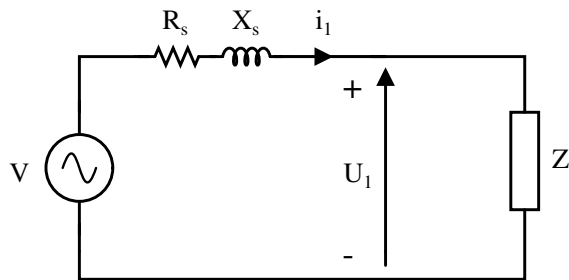


Figure 3.4: Effective circuit when switch S_1 is off

The equations for circuit in figure 3.4 are given below. By applying *KVL* to the loop, equation 3.1 is obtained.

$$V = (R_s + jX_s)i_1 + U_1 \quad (3.1)$$

$$U_1 = i_1 Z_l \quad (3.2)$$

The figure below shows the circuit diagram when the switch S_1 is on. Voltage at the *PCC* and system current when switch S_1 is on are assigned U_2 and i_2 . The current flowing through load is assigned i_3 .

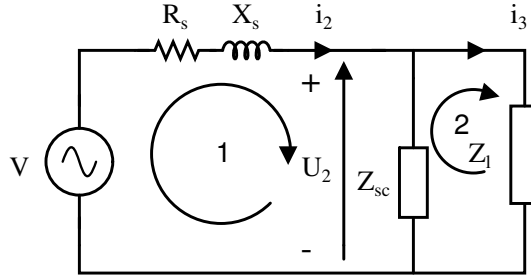


Figure 3.5: Effective circuit when switch S_1 is on

In circuit in figure 3.5 applying *KVL* for loop 1, we get

$$V = (R_s + jX_s)i_2 + (i_2 - i_3)Z_{sc} \quad (3.3)$$

For the same circuit, applying *KVL* for loop 2, we get following equation

$$\begin{aligned} i_3 Z_l + (i_3 - i_2)Z_{sc} &= 0 \\ \Rightarrow i_3 &= i_2 \left(1 + \frac{Z_l}{Z_{sc}}\right) \end{aligned} \quad (3.4)$$

By applying *KCL* at *PCC*, the current through Z_{sc} , $i_{Z_{sc}}$ flowing into Z_{sc} from the source can be written as

$$i_{Z_{sc}} = i_2 - i_3 \quad (3.5)$$

Voltage at *PCC*, U_2 is the voltage across Z_{sc} . Hence by Ohm's Law,

$$U_2 = i_{Z_{sc}} Z_{sc} \quad (3.6)$$

Substituting $i_{Z_{sc}}$ from equation 3.5

$$U_2 = (i_2 - i_3)Z_{sc} \quad (3.7)$$

Now, by substituting i_3 from equation 3.4

$$\begin{aligned} U_2 &= \left(i_2 - i_2 \left(1 + \frac{Z_l}{Z_{sc}} \right) \right) Z_{sc} \\ U_2 &= -i_2 Z_l \end{aligned} \quad (3.8)$$

Using equation 3.7 in equation 3.3, we get

$$V = (R_s + jX_s)i_2 + U_2 \quad (3.9)$$

As the voltage generated by generator is same irrespective of load variations, V in equations 3.1 and 3.9 are equal. So RHS of equations 3.1 and 3.9 are equated.

$$\begin{aligned} (R_s + jX_s)i_1 + U_1 &= (R_s + jX_s)i_2 + U_2 \\ (R_s + jX_s)(i_1 - i_2) &= U_2 - U_1 \\ \Rightarrow R_s + jX_s &= \frac{U_2 - U_1}{i_1 - i_2} \end{aligned} \quad (3.10)$$

As $Z_s = R_s + jX_s$,

$$\boxed{Z_s = \frac{U_2 - U_1}{i_1 - i_2}} \quad (3.11)$$

As the analysis is done in frequency domain, the above equation is valid for fundamental frequency. By assuming that the voltage generated by generator has only fundamental frequency, we can say that voltage generated at other frequencies is zero whether the switch S_1 is on or off. Hence by analyzing the same circuit for different frequencies will yield the same result, with the only difference being that V is zero. So, by transforming the voltage measured at PCC and current through the system to frequency domain, Z_s can be calculated at all the frequencies.

3.2 Signal Processing

The signals obtained are samples that are transformed into frequency domain for doing calculations in order to obtain frequency spectrum of impedance. The current and voltage signals obtained are converted into frequency domain by using Discrete Fourier Transform (*DFT*). The system is injected with harmonic currents and data is collected for one period in the disturbed state and for one period in normal state.

For a signal $x_{per}[n]$ which is periodic with period L where $n = 0, 1, 2, \dots, L - 1$, the signal can be converted to a finite-length signal $x[n]$ for calculating its *DFT* as follows:

$$x[n] = \begin{cases} x_{per}[n], & n = 0, 1, 2, \dots, L - 1 \\ 0, & \text{otherwise} \end{cases} \quad (3.12)$$

Now, for the finite length signal $x[n]$, the *DFT* coefficients are as follows:

$$X[k] = \sum_{n=0}^{L-1} x[n] e^{\frac{2\pi kn}{L}}, \quad k = 0, 1, 2, \dots, L - 1 \quad (3.13)$$

According to the sampling frequency F_s chosen, frequencies can be correlated to $X[k]$ samples chosen as follows:

$$f[k] = \frac{F_s}{2} \frac{k}{L}, \quad k = 0, 1, 2, \dots, L - 1 \quad (3.14)$$

where $f[k]$ are the frequencies corresponding to $X[k]$.

The above equations are used to obtain the frequency response of voltage and current from which equation 3.11 can be used to compute Z_s at each frequency $f[k]$ and hence impedance-frequency plot is obtained.

CHAPTER 4

SIMULATION FOR IMPEDANCE IDENTIFICATION OF GRID

The method explained in chapter 3 is implemented in simulations. For simulations, MATLAB[®] and MATLAB SIMULINK[®] are used. Firstly, circuits used for simulations are made in SIMULINK, and the voltage and current plots are obtained which are then transferred into MATLAB workspace. In MATLAB, the voltage and current data obtained are transformed into frequency domain by using *FFT* module, which efficiently calculates *DFT* of voltage and current. This data is used to calculate source impedance Z_s and the frequency plots of Z_s are plotted.

To verify the accuracy of measurements, different known filters are used and the changes in impedance plots are recorded. Then the changed plots are then compared to the ideal plots of source impedance by taking a thevenin equivalent of source from the obtained results.

4.1 Simulation Parameters

Simulations are done for different situations involving different sources and loads. The common simulation parameters for all kinds of sources and loads used are as follows:

- Solver used: ode3 fixed step solver at step size of 10^{-6} .
- Sampling frequency used is 1 *MHz*.

Parameters used when load is modelled in a way that it takes time in order of micro seconds to achieve stationary operation, system will reach steady-state immediately in simulation, and the following parameters are used:

- Simulation is run for 0.08 *s*, which is four periods.
- Disturbance is given for 1 *ms* at 0.05 *s*, i.e. when voltage crosses 0 *V* towards negative peak.

. When load is modelled so that it takes long time to reach steady-state, Disturbance is given and voltage and current data is collected only after the simulation reaches steady state, and hence the values of simulation parameters are dependent on how long the load takes to reach steady-state.

4.2 Simulation for a simple RL load

The circuit used here has a 230V voltage source with source impedance as shown in figure 4.1. The load used is a simple RL load with power ratings of 10KVA@0.8pf for 230V rated voltage.

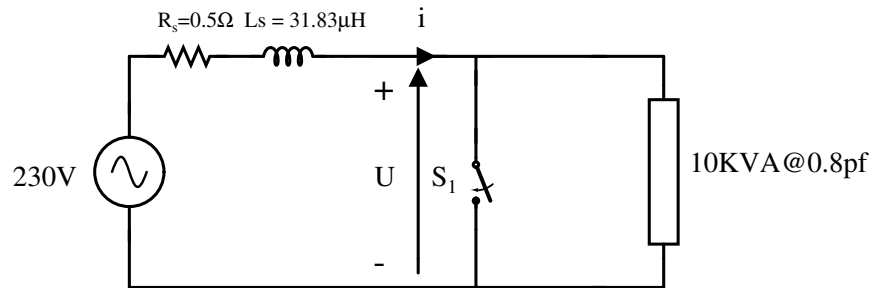


Figure 4.1: Circuit used for simulation

4.2.1 System results registered and Impedance Plots

For the circuit shown in figure 4.1, the voltage and current plots are as shown in the figures 4.2 and 4.3.

From the plots shown in the two figures shown below, we can see that with a low-impedance short, there is a disturbance in both voltage and current between 0.05 s and 0.051 s. This impulse is used to generate harmonics in the system.

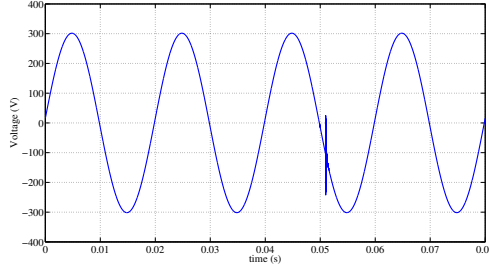


Figure 4.2: Voltage-time plot for RL load

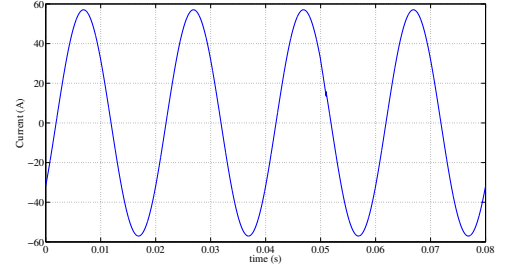


Figure 4.3: System current-time plot for RL load

Figure 4.4 shows the Frequency spectrum of impedance obtained by using equation 3.11. From the plot, it can be inferred that the source resistance is 0.5Ω and source reactance is an inductor, and its inductance L_s can be found out by the slope of the reactance versus frequency plot by using following equation:

$$L_s = \frac{m}{2\pi} \quad (4.1)$$

where m is the slope of reactance vs frequency plot.

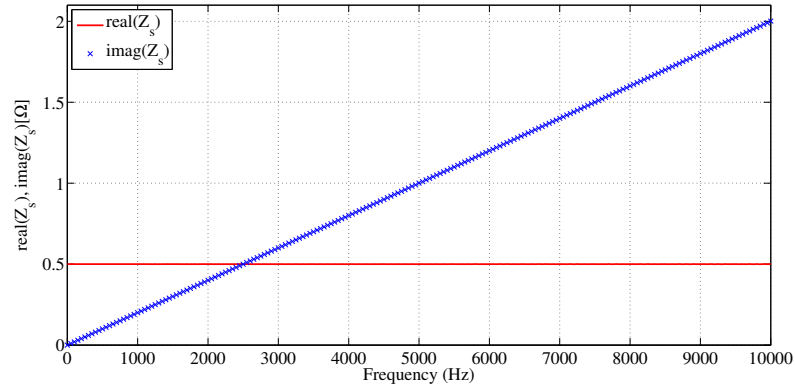


Figure 4.4: Frequency response of real and reactive source impedance values for RL load

Here, the slope of the reactance-frequency plot is

$$m = \frac{0.2 - 0}{1000 - 0}$$

$$m = 2 \times 10^{-4}$$

So from equation 4.1

$$\begin{aligned} \Rightarrow L_s &= \frac{2 \times 10^{-4}}{2\pi} \\ &= 3.183 \times 10^{-5} H \\ &= 31.83 \mu H \end{aligned}$$

4.2.2 Method Verification

For the purpose of verifying whether the obtained results are accurate, a few tests are done on the system which are as follows:

- Test impedance plots by using capacitive filter with leakage resistance.
- Test impedance plot by using LC filter.

Verification using Capacitor at PCC

For this verification, a capacitor with series leakage resistance is placed at the output of source as shown in following figure.

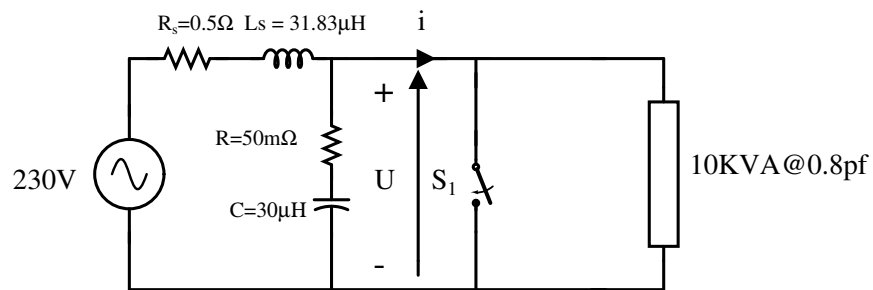


Figure 4.5: System with capacitor installed across the PCC

Impedance frequency responses are recorded as shown in the following figures.

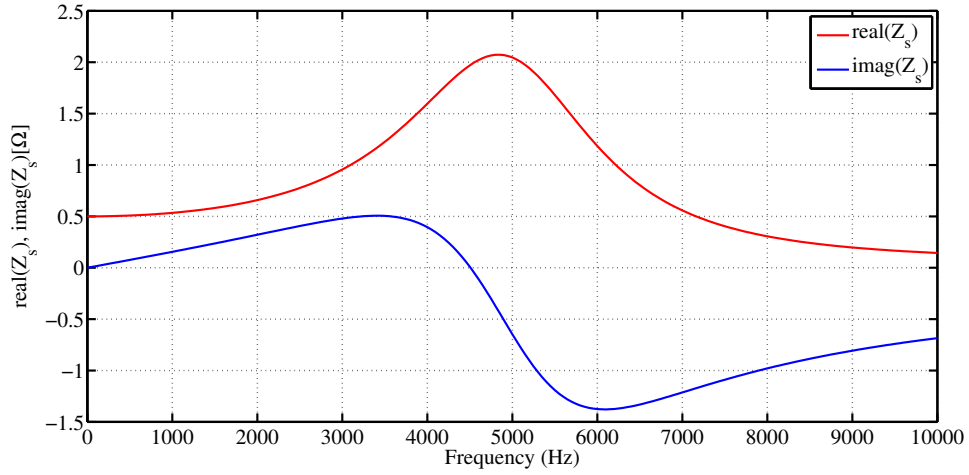


Figure 4.6: Frequency Response of real and reactive source impedance values with Capacitive filter at the *PCC*

The way to verify the correctness is to find out simple thevenin equivalent impedance of the source with respect to load. The load sees the source as a voltage source in parallel to a capacitor. For finding the thevenin equivalent impedance, the source is shorted and the the output impedance is found out as shown in the figure below.

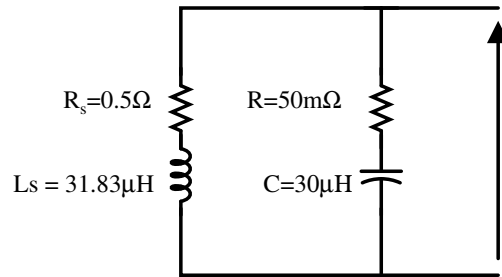


Figure 4.7: Thevenin equivalent impedance of system as seen by load

By using the impedance obtained in above circuit, impedance-frequency plot is obtained and is plotted in the figure below. This is used to verify correctness of the method.

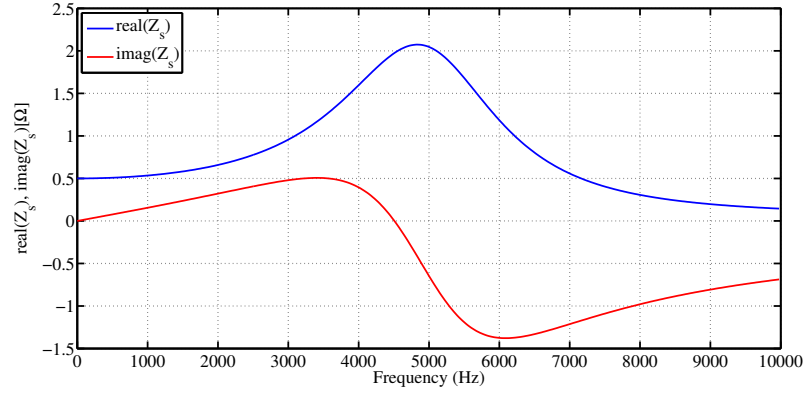


Figure 4.8: Ideal Frequency Response of real and reactive source impedance values for capacitive filter

Verification using LC filter at *PCC*

For this verification, an LC filter with series leakage resistance is placed at the output of source as shown in following figure.

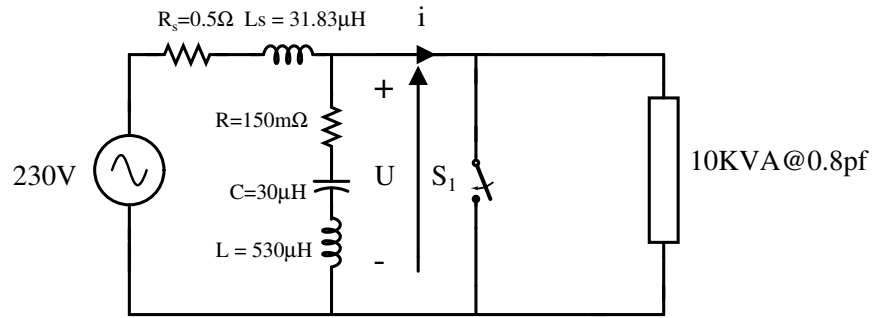


Figure 4.9: System with LC filter installed across the *PCC*

Impedance frequency responses are recorded as shown in the following figures.

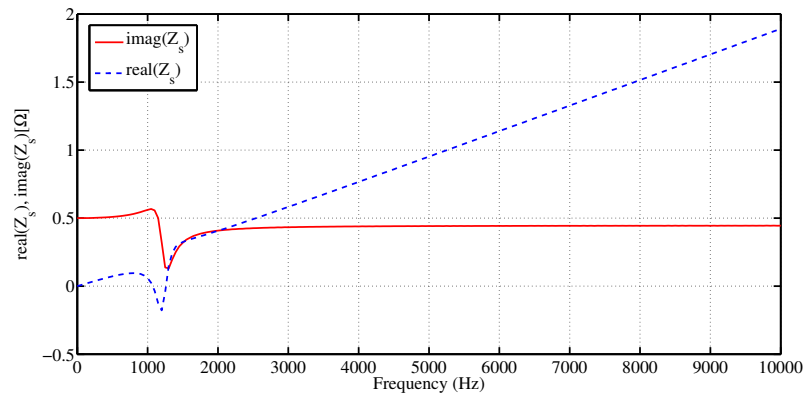


Figure 4.10: Frequency Response of real and reactive source impedance values with LC filter at the *PCC*

Thevenin equivalent impedance of source as seen by load can be calculated by using the circuit in figure 4.11. By using the impedance obtained in the circuit, impedance-frequency plot is obtained and is plotted in the figure below. This is used to verify correctness of the method.

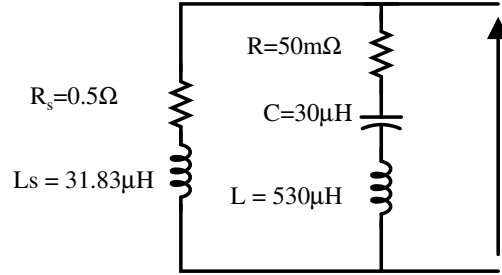


Figure 4.11: Thevenin equivalent impedance of system as seen by load

The plot obtained by using the equivalent impedance is shown in figure 4.12.

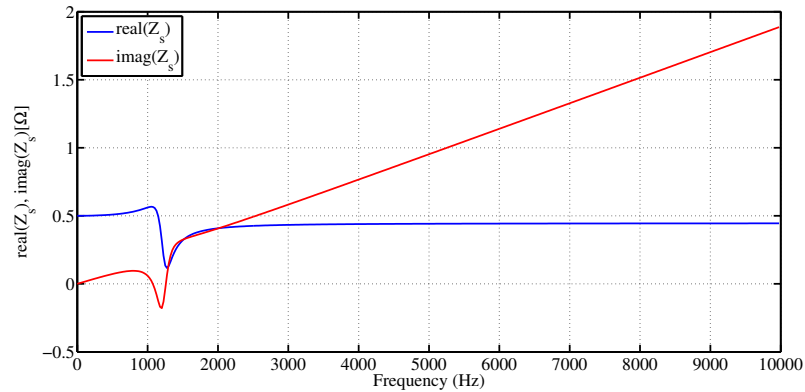


Figure 4.12: Frequency Response of impedance magnitude ideal plot with LC filter at the *PCC*

4.3 Simulations for LC parallel load

The load used for this simulation is an LC parallel load as shown in the figure below.

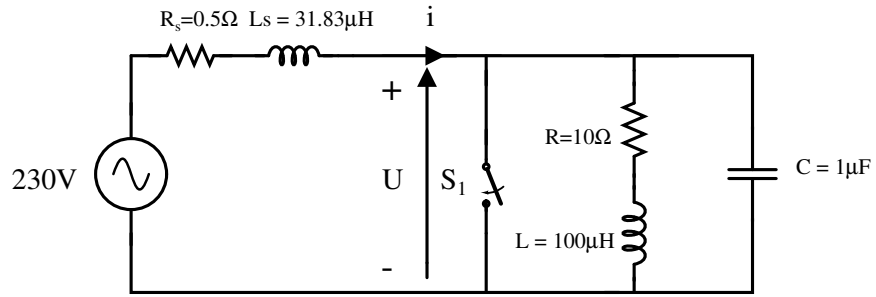


Figure 4.13: System with load as parallel combination of inductor and capacitor

The simulation results for the above circuit are shown in the following subsection.

4.3.1 System results registered and Impedance Plots

The current and voltage disturbances obtained are plotted in figure 4.14

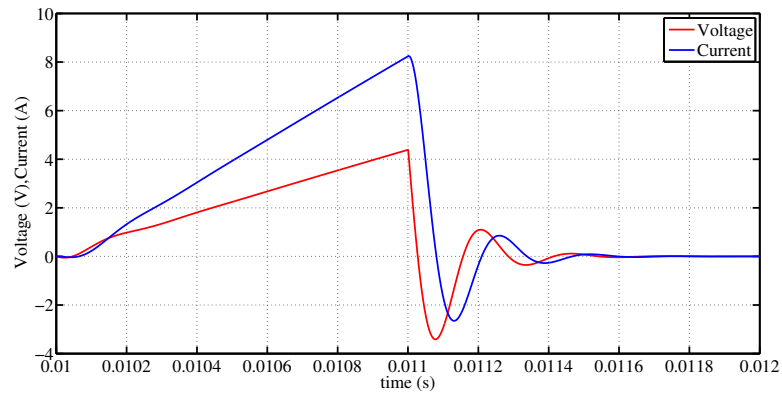


Figure 4.14: Voltage and current differences during disturbance vs time

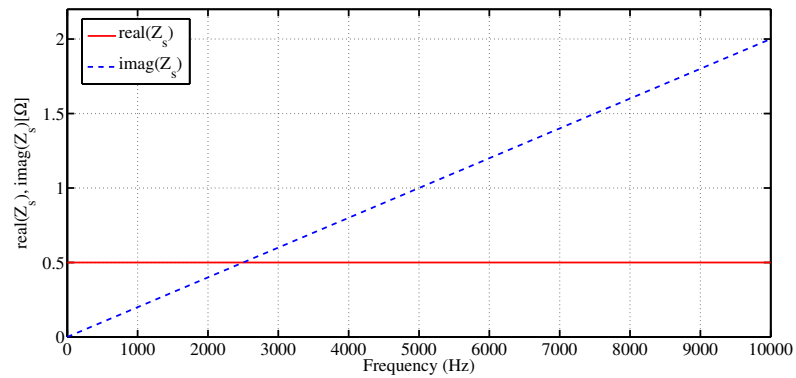


Figure 4.15: Frequency Response of real and reactive source impedance values for LC load

The impedance plot obtained is shown in figure 4.15. Source resistance obtained is 0.5Ω . The slope of source reactance plot is $m = (0.2 - 0)/(1000 - 0)$ and from equation 4.1, inductance is found out to be $31.83 \mu H$.

4.3.2 Method Verification

The results are verified by using same methods used in section 4.2.2.

Verification using Capacitor at *PCC*

The circuit used for verification is shown below.

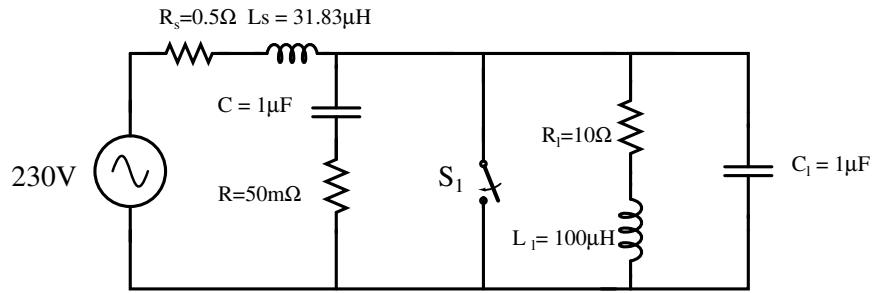


Figure 4.16: LC load with capacitor at *PCC*

For the above circuit, the impedance-frequency response obtained is shown below.

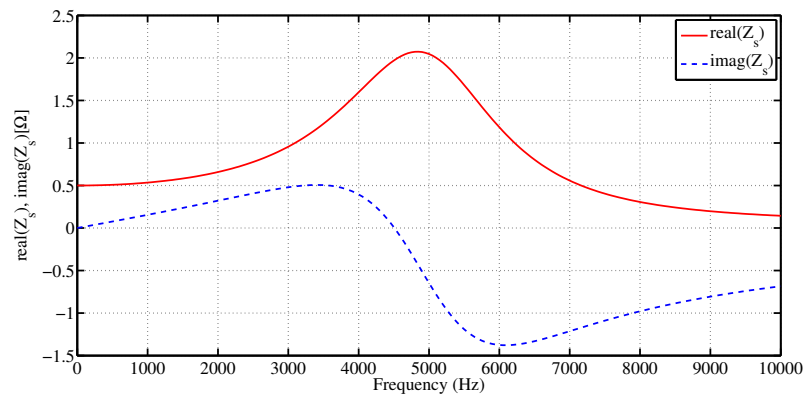


Figure 4.17: Frequency response of real and reactive source impedance values for LC load with capacitor at *PCC*

The Frequency response obtained is compared to the impedance response obtained from thevenin equivalent of source impedance at the *PCC* shown in figure 4.8 and it can be seen that the two plots match and hence the response obtained can be concluded as correct response.

Verification using LC filter at *PCC*

The circuit used for verification is shown below.

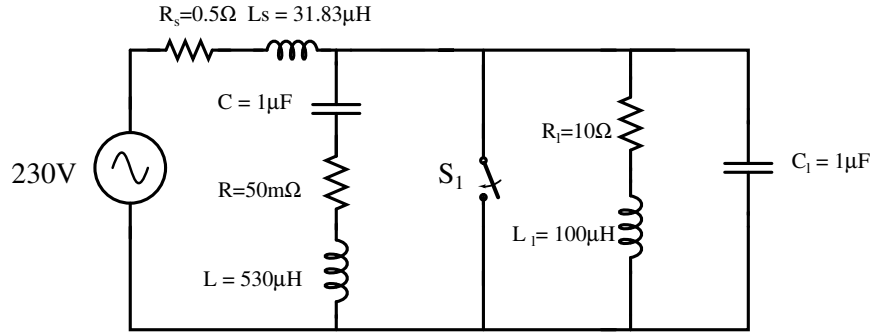


Figure 4.18: LC load with capacitor at *PCC*

For the above circuit, impedance-frequency response is shown in the figure below.

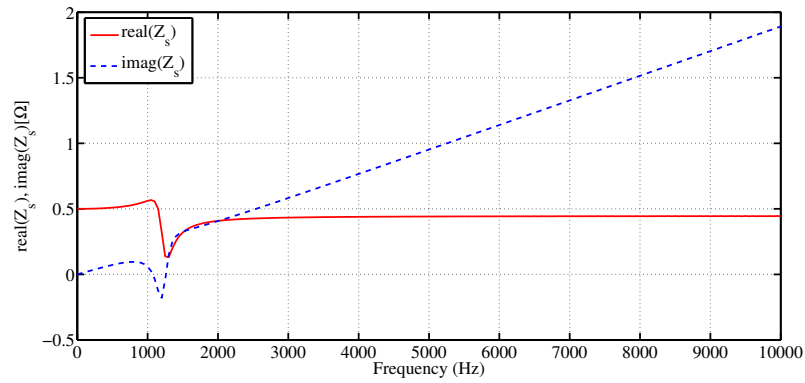


Figure 4.19: Frequency response of real and reactive source impedance values for LC load with LC filter at *PCC*

The Frequency response obtained is compared to the impedance response obtained from thevenin equivalent of source impedance at the *PCC* shown in figure 4.12 and it is found that the two plots match and hence the response obtained can be concluded as correct response.

4.4 Simulations for Permanent Magnet DC Motor

In order to verify whether the method is applicable for loads which generate harmonics, a permanent magnet DC machine is used which takes input from Rectifier circuit connected to the *PCC*. The circuit is as shown in the figure below.

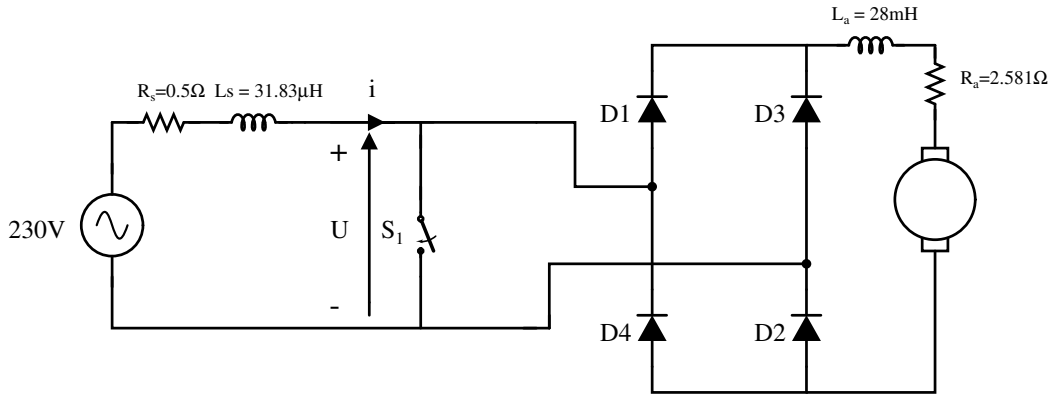


Figure 4.20: System loaded with a PMDC machine

The dc motor is run with constant speed of 50 rad/s . From observations, it is found out that the motor reaches steady-state operation in two seconds. Hence, the system observations and disturbance observations are recorded only after two seconds.

4.4.1 System results registered and Impedance Plots

The system is disturbed with a low-impedance short for 1 ms at simulation time 4.01 s . The voltage and current plots for the system are shown in following figures.

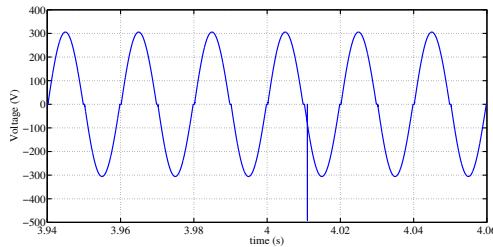


Figure 4.21: Voltage-time plot of system loaded with PMDC motor

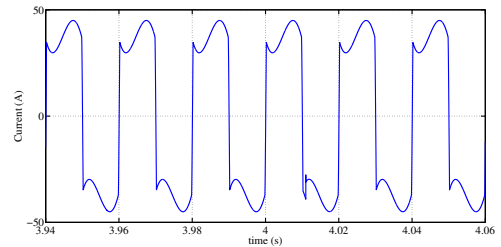


Figure 4.22: System-side current vs time plot for system loaded with PMDC motor

As the voltage is converted to DC, the current-time plot suddenly switches from positive peak to negative peak in a very short period of time for every cycle. The obtained current-time plot is shown below. *FFT* is taken for current and voltage disturbances and frequency response of impedance is obtained as shown in the figure below.

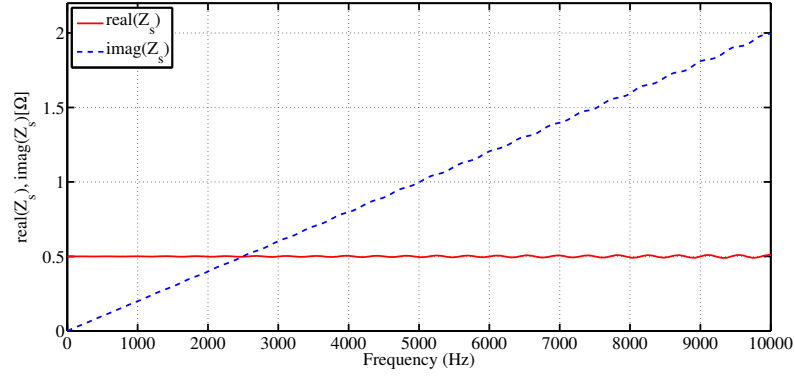


Figure 4.23: Frequency response of real and reactive source impedance values for system loaded with PMDC machine

From the above plot, it can be said that source resistance is 0.5Ω . The slope of source reactance plot is $m = (0.2 - 0)/(1000 - 0)$ and from equation 4.1, inductance is found out to be $31.83 \mu H$.

4.4.2 Method Verification

Verification using Capacitor at PCC

The following circuit is used for verifying the results. The Capacitor is connected in parallel to line output.

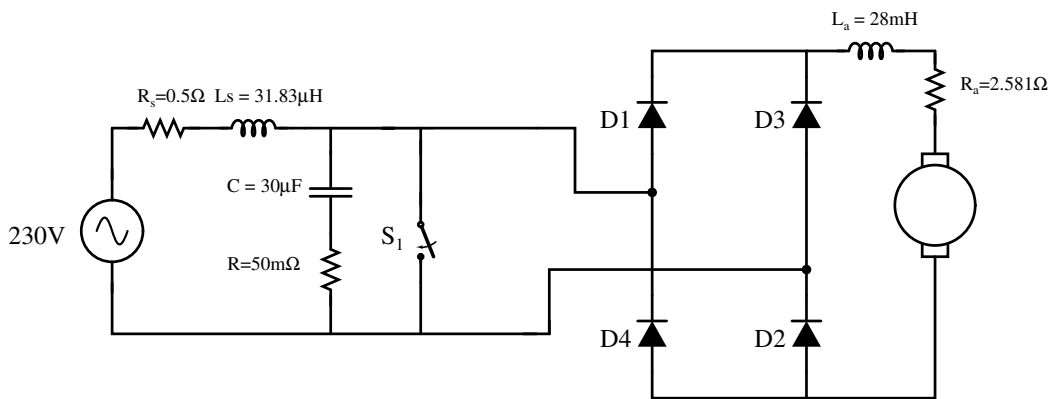


Figure 4.24: DC machine loaded system with capacitor at PCC

Frequency response of source impedance obtained is shown in figure below.

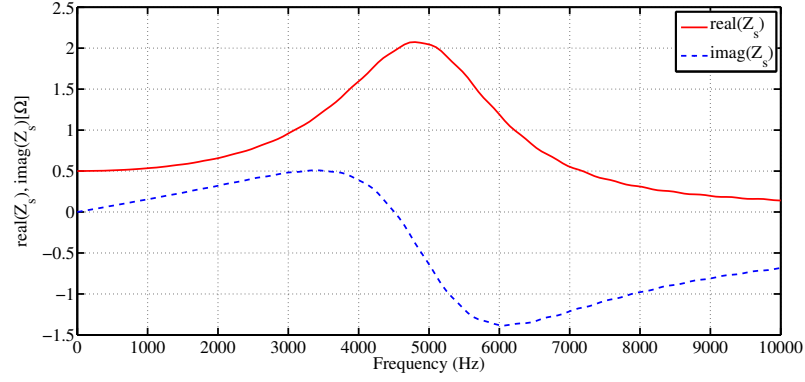


Figure 4.25: Frequency response of real and reactive source impedance values for system loaded with PMDC motor

The Frequency response obtained is compared to the impedance response obtained from thevenin equivalent of source impedance at the *PCC* shown in figure 4.8 and it is found that the two plots match and hence the response obtained is accurate.

Verification using LC filter at *PCC*

Following figure shows the circuit used for verification. The capacitor in circuit 4.24 is replaced by an LC filter.

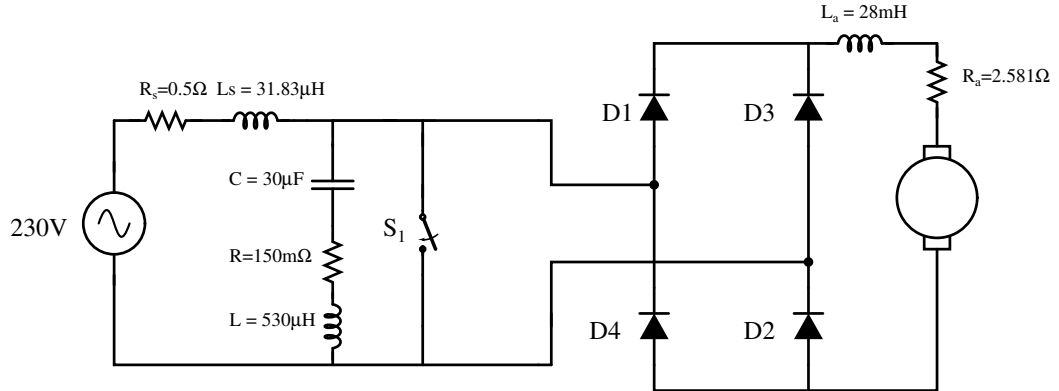


Figure 4.26: DC machine loaded system with LC filter at *PCC*

Frequency response of source impedance is shown in figure below.

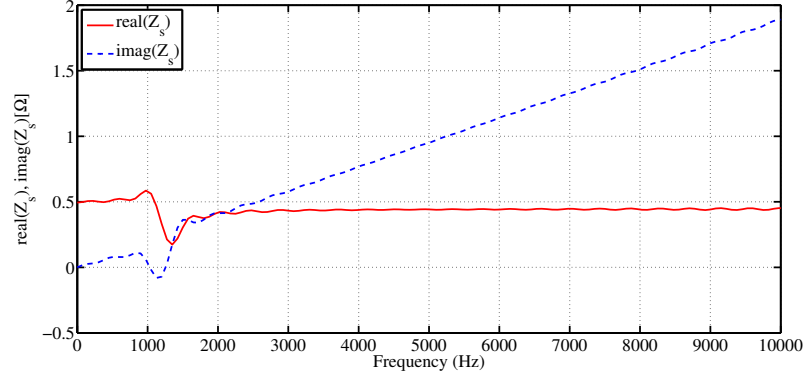


Figure 4.27: Frequency Response of real and reactive source impedance values for system loaded with PMDC machine and LC filter at *PCC*

The Frequency response obtained is compared to the impedance response obtained from thevenin equivalent of source impedance at the *PCC* shown in figure 4.12 and it is found that the two plots match and hence the response obtained can be concluded as correct response.

4.5 Simulation for a Three-bus System

The following single-line diagram shows a three-bus system taken from example 6.8 of Saadat (2002). Voltage and impedance values are given in per unit system and power is converted to per unit system with 100MVA base.

The load center in the figure below is bus 2 which consumes a real power of 400MW and reactive power of 250MVAR , and converting them to per unit using 100MVA base, the real power and reactive power are 4pu and 2.5pu respectively.

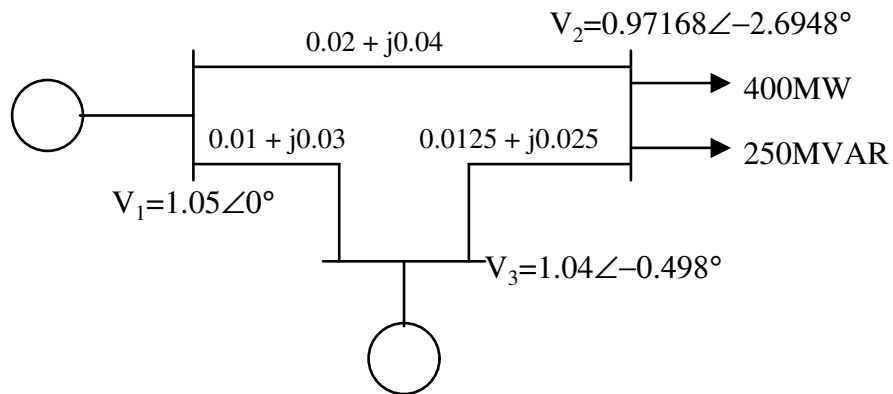


Figure 4.28: Single line model of three-bus system used for simulation

4.5.1 System results observed

The simulation circuit is shown below.

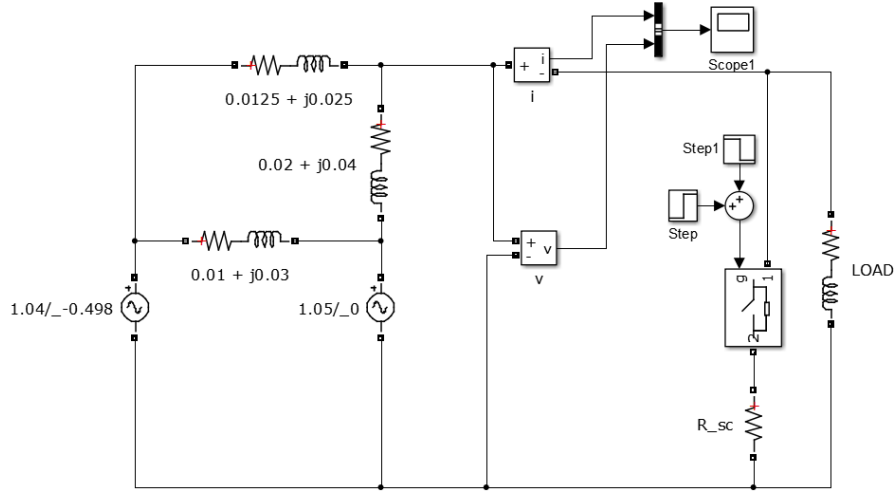


Figure 4.29: Simulation circuit for the three-bus system

For the circuit shown, source impedance plots obtained are shown in figure 4.30 and 4.31. The source resistance obtained from figure 4.30 is $7.69m\Omega$. The slope of reactance-frequency plot is $m = (0.3077 - 0)/(1000 - 0) = 30.77 \times 10^{-5}$. Hence, from equation 4.1, $L = 48.97\mu H$.

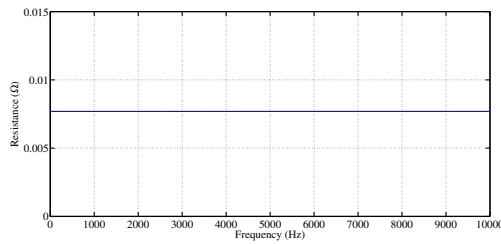


Figure 4.30: Frequency Response of source resistance for three-bus system

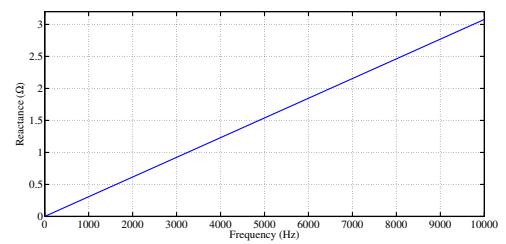


Figure 4.31: Frequency Response of source reactance for three-bus system

4.5.2 Method Verification

For verification, the following simulink circuit is used where the verifying circuits are connected between node 1 and node 2.

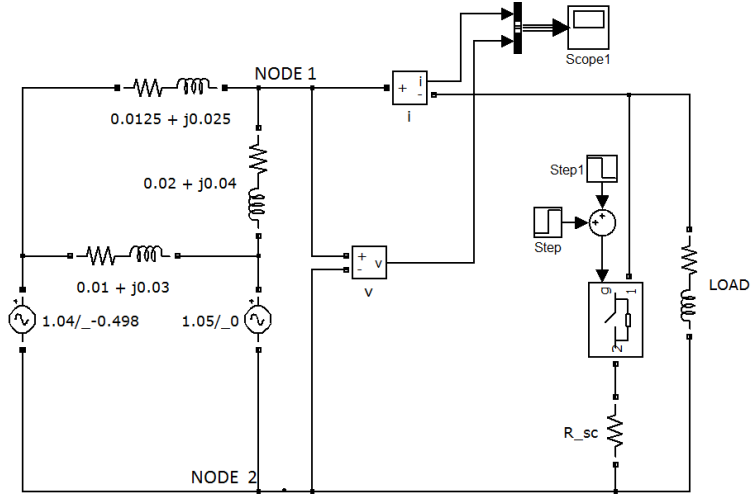


Figure 4.32: Simulation circuit for verification of correctness of impedance for three-bus

Verification using capacitor at *PCC*

A capacitor of value $100\mu F$ with a leakage resistance of $150m\Omega$ is connected between node 1 and node 2 of figure 4.32. The circuit is now simulated to obtain frequency response of impedance.

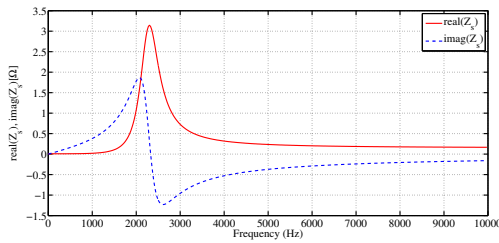


Figure 4.33: Frequency Response of real and reactive source impedance for capacitive loading at *PCC*

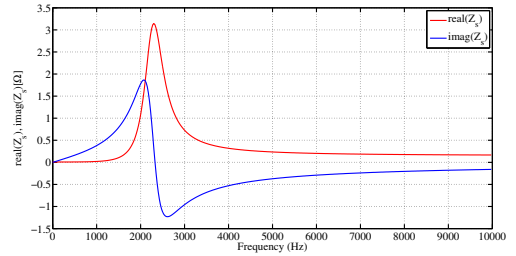


Figure 4.34: Ideal Frequency Response of real and reactive source impedance for capacitor loading at *PCC*

The thevenin equivalent impedance of the source as seen by load at *PCC* is obtained by using the source impedance obtained in section 4.5.1 and the capacitor connected. Source impedance-frequency plot is obtained using this method is used to verify the frequency response found out by using low-impedance short-circuiting method.

Verification using LC filter at PCC

A LC filter with inductance of $50\mu H$ and capacitance of $100\mu F$ with a leakage resistance of $150m\Omega$ is connected between node 1 and node 2 of figure 4.32. The circuit is now simulated to obtain frequency response of impedance.

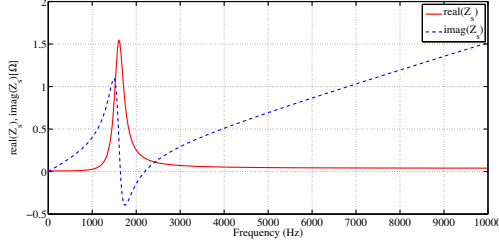


Figure 4.35: Frequency Response of real and reactive impedance for LC loading at PCC

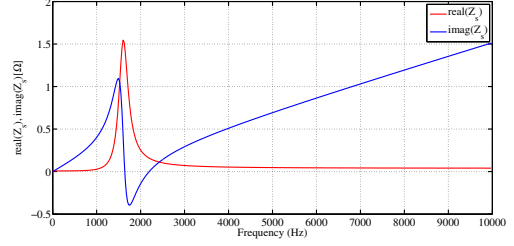


Figure 4.36: Ideal Frequency Response of real and reactive source impedance for LC loading at PCC

The thevenin equivalent impedance of the source as seen by load at PCC is obtained by using the source impedance obtained in section 4.5.1 and the LC filter connected. Source impedance-frequency plot is obtained using this method is used to verify the frequency response found out by using low-impedance short-circuiting method.

CHAPTER 5

SIMULATION OF SYSTEM DISTURBANCES AND POWER QUALITY MEASUREMENT

In this chapter, different system disturbances are created and the effect of disturbances on change in power quality is observed and noted. It can be observed that by artificially creating these kind of system disturbances, we can also obtain the grid impedance.

Power quality is measured by means of Total Harmonic Distortion(THD) which indicates distortion level relative to the fundamental component of signal. If the rms value of current signal measured is I , then THD of the signal in percentage is given by

$$THD = \frac{\sqrt{I_2^2 + I_3^2 + I_4^2 + \dots + I_n^2}}{I_f} \times 100 \quad (5.1)$$

where I_n is RMS value of harmonic n

and I_f is RMS value of fundamental frequency

5.1 Simulation of Voltage Swell

Voltage swell phenomenon where there is a sudden increase in voltage for 4-5 cycles and normal operation is resumed after 4-5 cycles. Here voltage swell is created by artificially increasing the load for 5 cycles and by decreasing load to its previous state after 5 cycles. The voltage and current signals are shown in the figures below.

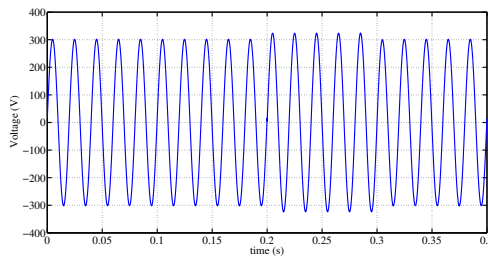


Figure 5.1: Voltage swell caused by sudden decrease of load

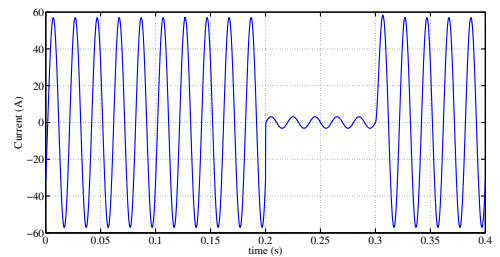


Figure 5.2: Current change caused by voltage swell

The voltage swell can be seen from time $0.2s$ to $0.3s$. The THD values for voltage and current are shown below:

Table 5.1: Voltages and current THD percentages during normal operation and during swell

	Voltage THD	Current THD
Normal Operation	9.069×10^{-3}	9.069×10^{-3}
During Swell	9.054×10^{-3}	9.069×10^{-3}

For voltage swell, by using equation 3.11, impedance-frequency response is obtained as shown in the figure below.

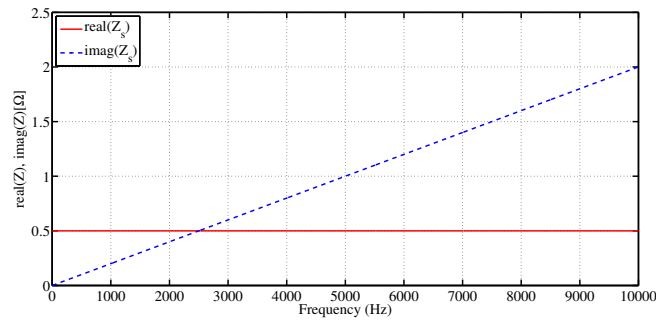


Figure 5.3: Frequency response of impedance found by using voltage swell method

From the above plot, it can be said that source resistance is $R_s = 0.5 \Omega$. The slope of source reactance plot is $m = (0.2 - 0)/(10000 - 0)$ and from equation 4.1, inductance is $L_s = 31.83\mu H$.

5.2 Simulation of Voltage Sag

Voltage sag phenomenon where there is a sudden decrease in voltage for 4-5 cycles and normal operation is resumed after 4-5 cycles. Here voltage sag is created by artificially reducing the load for 5 cycles and by increasing load to its previous state after 5 cycles. The voltage and current signals are shown in the figures below.

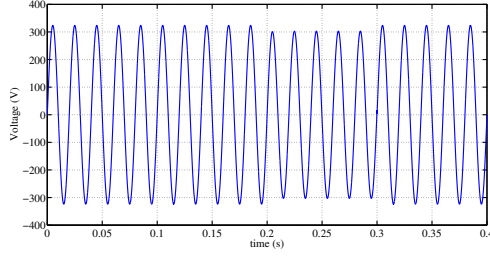


Figure 5.4: Voltage sag caused by sudden decrease of load

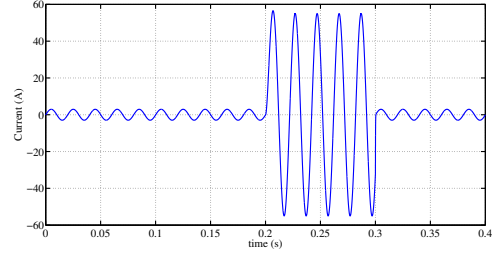


Figure 5.5: Current change caused by voltage sag

The voltage sag can be seen from time $0.2s$ to $0.3s$. The THD values for voltage and current are shown below:

Table 5.2: Voltages and current THD percentages during normal operation and during sag

	Voltage THD	Current THD
Normal Operation	9.069×10^{-3}	9.069×10^{-3}
During Sag	9.069×10^{-3}	9.069×10^{-3}

For voltage sag, by using equation 3.11, impedance-frequency response is obtained as shown in the figure below.

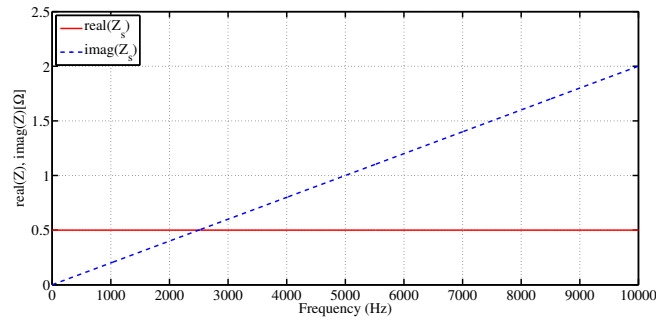


Figure 5.6: Frequency response of impedance found by using voltage sag method

From the above plot, it can be said that source resistance is $R_s = 0.5 \Omega$. The slope of source reactance plot is $m = (0.2 - 0)/(10000 - 0)$ and from equation 4.1, inductance is $L_s = 31.83 \mu H$.

5.3 Simulation for disturbance by adding sudden RL load to a DC motor system

System here drives a DC motor through a full-bridge rectifier. This system has switched current waveform and hence has high THD . This system is additionally loaded with RL load in parallel to the DC motor system for a short time and then removed. Voltage and current signals are shown in the figures below.

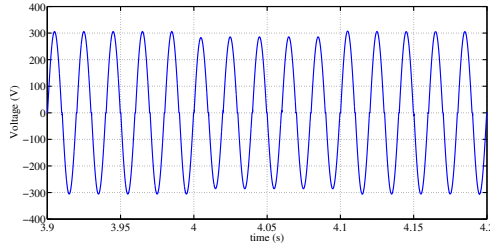


Figure 5.7: Voltage change caused by sudden RL switching on motor load

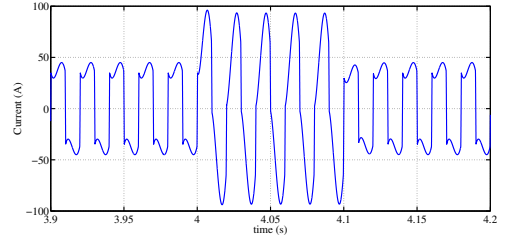


Figure 5.8: Current change caused by sudden RL switching on motor load

Voltage and current THD values when system is loaded with RL load and during normal operation are shown in the following table.

Table 5.3: Voltages and current THD percentages during normal operation and when loaded with extra RL load

	Voltage THD	Current THD
Normal Operation	3.45	41.94
Loaded with Extra RL load	3.191	18.95

For RL loading of system with DC motor, by using equation 3.11, impedance-frequency response is obtained as shown in the figure below.

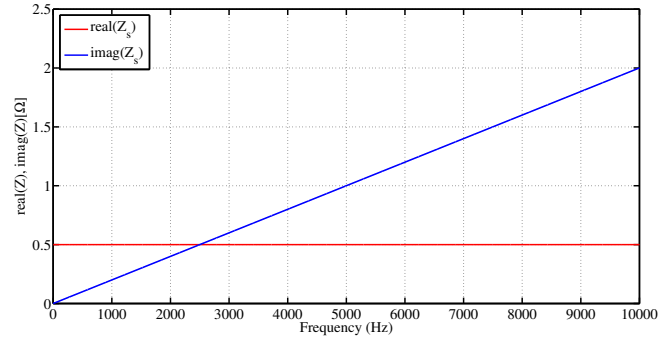


Figure 5.9: Frequency response of impedance found by sudden RL switching on motor load

From the above plot, it can be said that source resistance is $R_s = 0.5 \Omega$. The slope of source reactance plot is $m = (0.2 - 0)/(1000 - 0)$ and from equation 4.1, inductance is $L_s = 31.83 \mu H$.

CHAPTER 6

CONCLUSIONS

6.1 Conclusion

By using the method used in Staroszczyk (2005) as a reference, a new method for grid impedance identification has been found out. The new method is used and grid impedance has been identified for a frequency spectrum from $0Hz$ to $10kHz$ for different kinds of loads by using a single source. The method is also tested for a three-bus system with two sources supplying a same load and the obtained results are verified by adding different impedances in parallel to the source, and the results are as expected.

Different system disturbances are also created by using switched loads, sudden load changes, etc. and the power quality analysis has been done for the created disturbances. Source impedance has also been found out with the help of the disturbances created.

6.2 Future Work

In the method used for impedance identification, filters can be introduced and the sampling frequency for measuring signals can be reduced. A grid impedance identification tool can be implemented, which can be portable and can measure real-time grid impedance.

REFERENCES

1. **Staroszczyk, Z.**, *A Method for Real-Time, Wide-Band Identification of the Source Impedance in Power Systems*. IEEE Transactions on Instrumentation and Measurement, Vol. 54, No. 1, February 2005
2. **Bollen, M., Haesen, E., Minne, F., Dreisen, J.** *Hosting Capacity for Motor Starting in Weak Grids*. IEEE International conference on Future Power Systems, November 2005
3. **Soenke Grunau, Friedrich W. Fuchs** *Effect of Wind-Energy Power Injection into Weak Grids*. EWEA Proceedings, April 2012.
4. **N. P. W. Strachan, and Jovcic, D.** *Stability of a variable speed permanent magnet wind generator with weak ac grids*. IEEE Transactions on Power Delivery, Vol.25, No. 4, pp. 2779 – 2788, 2010
5. **Saadat, H.**, *Power System Analysis*. Tata McGraw-Hill, 2002